SCIENTIFIC PAPERS
OF THE UNIVERSITY OF PARDUBICE
Series B
The Jan Perner Transport Faculty
**18** (2012)

# STRENGTH CONTROL OF THE HOOD OF DIESEL ELECTRIC LOCOMOTIVE

Petr TOMEK, Doubravka STŘEDOVÁ

Department of Mechanics, Materials and Machine Parts

## 1. Introduction

The original structural design of hood is analyzed in this paper. The whole construction is loaded by force caused by the weight of the structure. The parts of the hood are subject to the standards for railway applications ČSN EN 12663-1 [1]. Numerical analyses are performed by FEM computer program COSMOSWorks [2]. The main aim of this paper is to determine critical points of construction on the basis of the results of numerical analyses. The critical points are expected in locations of welds tubes profiles.

The strength of hood is evaluation by two methods. The first methodology is anchored in ČSN EN 12663-1 [1]. The second methodology is nonlinear numerical analysis GMNA (Geometrically and Materially Nonlinear Analysis). The second methodology is applied to basis of methods of modern science and technology. The results are evaluated according to ČSN EN 12663-1 [1] and ČSN 73 1401 [3]. The influence of other loads is solved using the methods of modern science and technology.

## 2. Coordinate system and loads

The coordinate system is taken from ČSN EN 12663-1 (see Fig. 1). Numerical models are subjected to acceleration in specified directions. Acceleration values are given in Tab. 1.


***Fig. 1:*** *Coordinate system according to ČSN EN 12663–1 [1].*

***Tab. 1:*** *The limit value of acceleration for strength solution according to ČSN EN 12663–1 [1] (g=-9.81m/s$^2$).*

| *Load Case LC* | *acceleration in the **x**-axis* | *acceleration in the **y**-axis* | *acceleration in the **z**-axis* |
|---|---|---|---|
| 1+ | 0 | 0 | 3·g |
| 1 - | 0 | 0 | -1·g |
| 2+ | 3·g | 0 | 0 |
| 2 - | -3·g | 0 | 0 |
| 3+ | 0 | 1·g | 0 |
| 3 - | 0 | -1·g | 0 |
| 4+ | 3·g | 0 | 1·g |
| 4 - | -3·g | 0 | 1·g |
| 5+ | 0 | 1·g | 1·g |
| 5 - | 0 | -1·g | 1·g |

## 3. Numerical solution

Two methods are used to evaluate the strength of the hood. The first methodology anchored in ČSN EN 12663-1 [1] is based on a linear static analysis. Calculated pseudo - elastic stresses are compared with allowable stress. This methodology does not assess correctly the influence of stress concentrations (notches, changes in geometry, etc.) for strength of construction and it cannot detect any loss of stability. Results obtained from by method according to ČSN EN 12663-1 [1] are only approximate. The definite conclusion cannot be derived from these results. Detailed description of the first methodology anchored in ČSN EN 12663-1 [1] is given in Chap. 5$^{th}$.

The second methodology is applied to basis of methods of modern science and technology. Geometrically and materially nonlinear analysis (GMNA) is the basis of the second methodology. The real limit state (loss of stability, plasticity limit state) is the result of non-linear numerical analysis. The strength of construction is evaluated from the limit load, when it occur the real limit state. This method is commonly used for the design of restricted equipment (e.g. pressure vessels, steel structures, etc.) in the energy, chemical, nuclear and transportation industries. Detailed description of the second methodology is given in Chap. 6$^{th}$.

## 4. Material

***Tab. 2:*** *Mat. S275J2H – Mechanical properties.*

| *T* [°C] | *E* [MPa] | $R_{p0.2}$ [MPa] | $R_m$ [MPa] |
|---|---|---|---|
| 20 | 2.01E+5 | 275 | 430 |

## 5. Linear elastic numerical analyses

Methodology specified in ČSN EN 12663-1 [1] is used for evaluation of strength of the hood in this chapter. Methodology anchored in ČSN EN 12663-1 [1] is based on evaluation of the results the linear static analysis. Calculated pseudo - elastic stresses are compared with allowable stress. Allowable stress is determined by following condition:

$$\sigma_{ALL} = min\left(\frac{R_{p0,2}^{20}}{S_1};\frac{R_m^{20}}{S_2}\right) = min\left(\frac{275}{1.15};\frac{430}{1.5}\right) = min(239.13\,;286.67) = 239.13\ MPa$$

Where

$S_1$=*1.15* – Safety factor given the yield stress,

$S_2$=*1.5* – Safety factor given the yield strength.

$$\boldsymbol{\sigma_{ALL} \doteq 239\ MPa}$$

Equivalent (reduced) stress according to the hypothesis of maximum shear stress (Tresca, intensity) $\sigma_{int}$ is used for evaluation of strength. Standard ČSN EN 12663-1 [1] does not distinguish surface of the shell element (TOP, MIDDLE, BOTTOM). Stress is conservatively evaluated on the surfaces TOP and BOTTOM.

Conditions of strength according to ČSN EN 12663-1 [1] are:

1. The calculated stress in the numerical model $\sigma_{int}$ cannot exceed the allowable stress $\sigma_{ALL}$ = 239 MPa.
2. Calculated pseudo - elastic stress can be exceed yield stress $R_{p0,2}$=275 MPa in the local stress concentrations. Areas with permanent deformations due to local stress concentrations must be sufficiently small. Significant permanent deformation cannot occur after the end of the load.

The computational model of hood is a large and difficult. The individual connections of tubes (structural nodes) are evaluated separately. Identification of all connections is shown on the Fig. 2, Fig. 3 and Fig. 4.

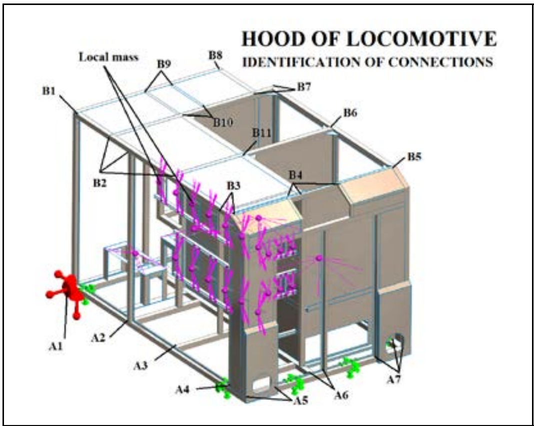


***Fig. 2:*** *Identification of connections.*

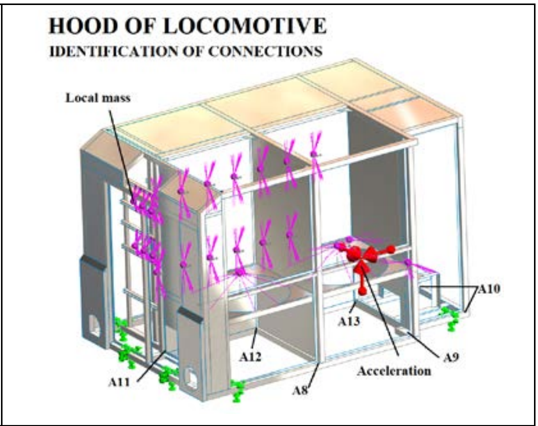


***Fig. 3:*** *Identification of connections.*

The mesh is always softened at controlled connection. The rest of construction contains a loose mesh. For each connections and selected load cases (Tab. 1) were performed numerical linear static analyses. Example of evaluation connections A9 and B10 for load case LC = 1+ follows.

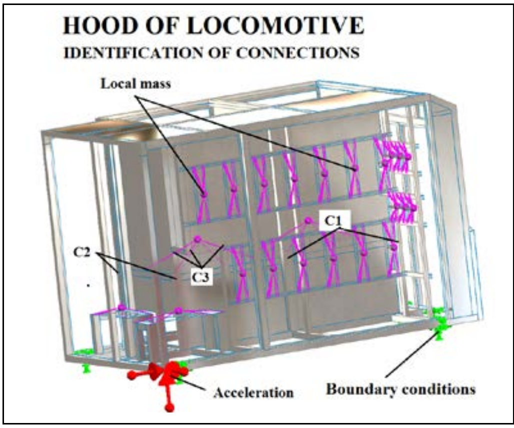


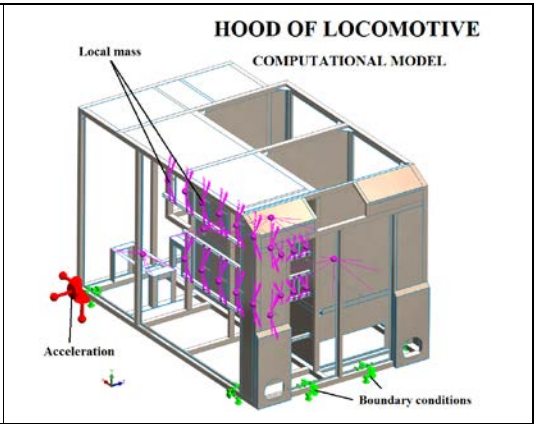


***Fig. 4:*** *Identification of connections.* ***Fig. 5:*** *Computational model.*

The computational model is shown in Fig. 5. FEM mesh is created by parabolic shell-elements SHELL6T (Fig. 6 and Fig. 8). Deformed model with-drawn a reduced stress Tresca on the TOP surface is shown in Fig. 7 and Fig. 9. The red (dark)-colored areas are clearly visible on the numerical model. The reduced stress $\sigma_{intz}$ exceeded the allowable stress $\sigma_{ALL}$ = 239 MPa in this areas. The results are summarized in Tab. 3, Tab. 4 and Tab. 5.

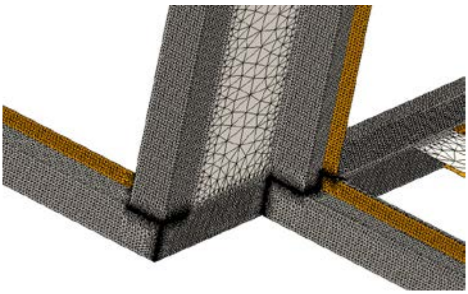

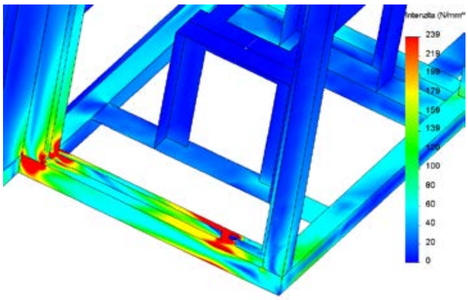

***Fig. 6:*** *A9 – FEM Mesh.* ***Fig. 7:*** *A9 – Reduced stress Tresca.*

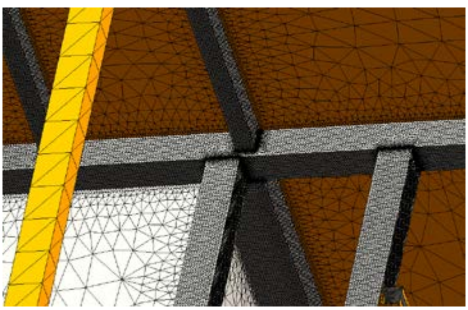

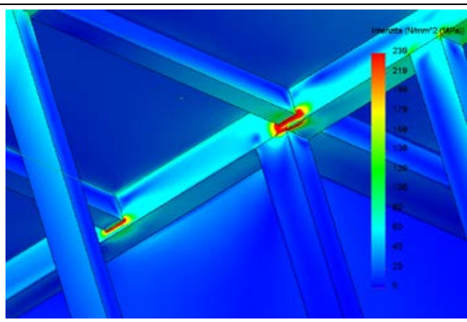

***Fig. 8:*** *B10 – FEM Mesh.* ***Fig. 9:*** *B10 – Reduced stress Tresca.*

***Tab. 3:*** Evaluation *of strength–Bottom part of the hood.*

| Identification of connection | *Load Case LC=1+* | *Load Case LC=2+* |
|---|---|---|
| A1 | SATISFIES | SATISFIES |
| A2 | SATISFIES | SATISFIES |
| A3 | SATISFIES | SATISFIES |
| A4 | **DOES NOT SATISFY** | **DOES NOT SATISFY** |
| A5 | SATISFIES | SATISFIES |
| A6 | SATISFIES | **DOES NOT SATISFY** |
| A7 | **DOES NOT SATISFY** | **DOES NOT SATISFY** |
| A8 | SATISFIES | SATISFIES |
| A9 | **DOES NOT SATISFY** | **DOES NOT SATISFY** |
| A10 | **DOES NOT SATISFY** | SATISFIES |
| A11 | SATISFIES | SATISFIES |
| A12 | SATISFIES | SATISFIES |
| A13 | SATISFIES | SATISFIES |

***Tab. 4:*** Evaluation *of strength–Middle part of the hood*

| Identification of connection | *Load Case LC=1+* |
|---|---|
| C1 | SATISFIES |
| C2 | SATISFIES |
| C3 | SATISFIES |

***Tab. 5:*** Evaluation *of strength–Top part of the hood*

| Identification of connection | *Load Case LC=1+* | *Load Case LC=2+* | *Load Case LC=3+* |
|---|---|---|---|
| B1 | SATISFIES | SATISFIES | SATISFIES |
| B2 | SATISFIES | SATISFIES | SATISFIES |
| B3 | SATISFIES | SATISFIES | SATISFIES |
| B4 | SATISFIES | SATISFIES | SATISFIES |
| B5 | SATISFIES | SATISFIES | SATISFIES |
| B6 | SATISFIES | SATISFIES | SATISFIES |
| B7 | **DOES NOT SATISFY** | **DOES NOT SATISFY** | SATISFIES |
| B8 | SATISFIES | SATISFIES | SATISFIES |
| B9 | **DOES NOT SATISFY** | **DOES NOT SATISFY** | SATISFIES |
| B10 | **DOES NOT SATISFY** | **DOES NOT SATISFY** | SATISFIES |
| B11 | SATISFIES | **DOES NOT SATISFY** | SATISFIES |
| B12 | SATISFIES | SATISFIES | SATISFIES |

## 6. Nonlinear numerical analysis GMNA

Two nonlinearities are considered in numerical analyses.

- Geometric nonlinearity
- Material nonlinearity.

Geometric nonlinearity (large displacements) allows for the detection the loss of stability of the structure. Material nonlinearity takes into account elastic - plastic material behavior (plasticity). The von Mises´s bilinear model of elastic - plastic material behavior is considered in the numerical analyses GMNA. The evaluation construction for selected load cases follows.

### Vertical acceleration $a_z$ = 29.43 m/s$^2$ (LC 1+)

The limit acceleration of the numerical model is found in this chapter. The computational model is shown in Fig. 10. FEM mesh is created by shell element

SHELL3T (Fig. 11). The numerical model is exposed to acceleration $a_z=3\cdot g=29.43\ m.s^{-2}$ $(g=9.81\ m.s^{-2})$. Additional load of connecting parts are neglected. The equilibrium curve (see Fig. 12) is the ratio of the load factor LF (load multiple of computational load) in the total displacement of the selected nodes ND_18125 (Fig. 12). The numerical model has a linear behavior until the load factor *LF ~ 0.8.* Plastic hinges begin to develop after reaching this point. Establishment and development of plastic hinges is accompanied by a decrease stiffness of the construction. Limit state of plasticity is reached in the 55th step. The value of limit load factor is $LF_L$ = 1.74. The geometric nonlinearity was taken into account in solution (large displacements). The loss of stability was not indicated. Deformed model with drawn reduced stress von Mises on the top surface is shown in Fig. 13 and Fig. 14. The location of plastic hinges is clearly visible (the area where reduced stress reached the yield stress of material). Evaluation of the results follows.

Limit acceleration

$$a_{zL} = LF_L \cdot a_z = 1.74 \cdot 29.43 = 51.21\ m.s^{-2}$$

Allowable acceleration

$$a_{zALL} = \frac{a_{zL}}{S_f} = \frac{51.21}{2} = 25.61\ m.s^{-2}$$

where $S_f = 2$ … fictitious safety factor at yield strength

***Note:*** The fictitious safety factor $S_f$ takes into account plasticity and a thin wall profiles [4].

Strength condition

$a_z = 29.43\ m.s^{-2} \quad \nleq \quad a_{zALL} = 25.61\ m.s^{-2}$ -----> Does not satisfy !!!

**<u>The calculation result shows that the hood is not properly designed and it does not satisfy on the calculation load case $a_z$=29.43 m.s$^{-2}$ (*LC=1*+)</u>**

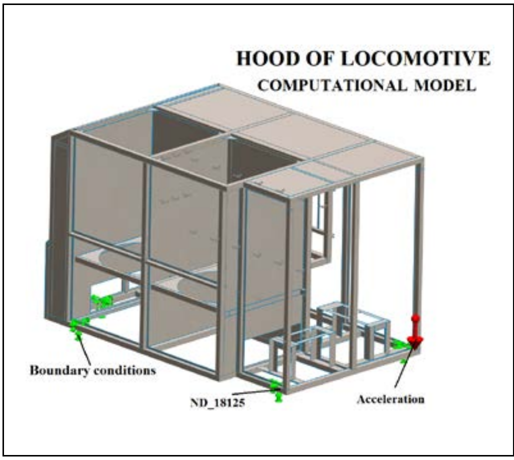


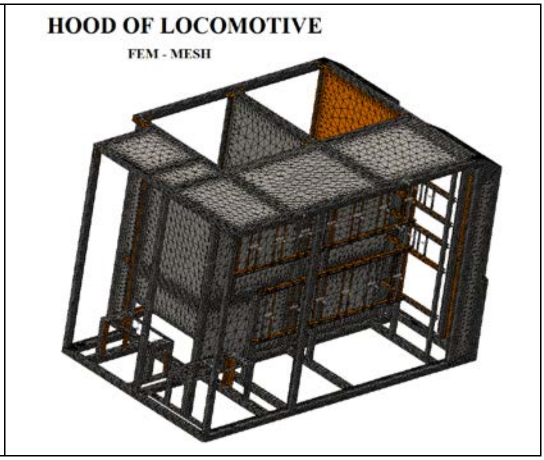


***Fig. 10:*** *Numerical model – LC 1+.*

***Fig. 11:*** *FEM mesh – LC 1+.*

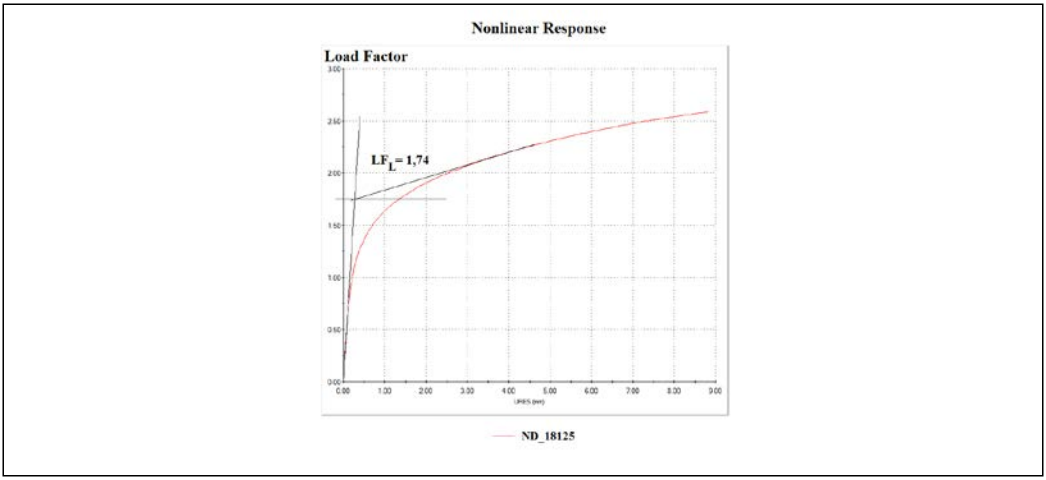


***Fig. 12:*** *Equilibrium curve – LC 1+.*

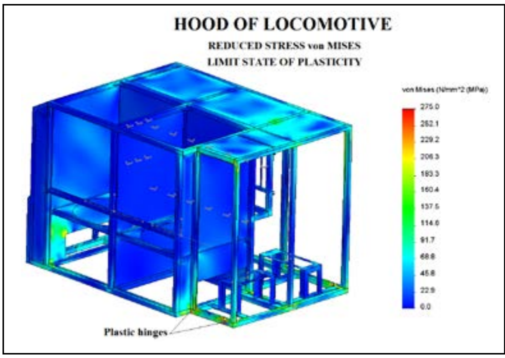


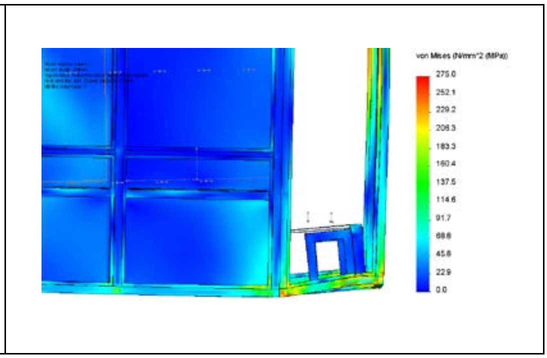


***Fig. 13:*** *Reduced stress Misses–LC 1+.*

***Fig. 14:*** *Detail of plastic hinges–LC 1+.*

## Lateral acceleration $a_y$ = 9.81 m/s$^2$ (LC 5+)

Results and evaluation of the strength of hood for the lateral acceleration are shown in this chapter. Detailed description of numerical analysis and evaluation of the strength is presented in chapter vertical acceleration (previous chapter). The limit acceleration of the numerical model is found in this chapter. The computational model is shown in Fig. 15. FEM mesh is created by shell element SHELL3T (Fig. 16). The numerical model is exposed to acceleration $a_z=1 \cdot g=9.81\ m.s^{-2}$ *and* $a_y=1 \cdot g=9.81\ m.s^{-2}$. Limit state of plasticity is reached in the 45$^{th}$ step. The value of limit load factor is $LF_L$ = 2.64 (see equilibrium curve in Fig. 17). Deformed model with drawn reduced stress von Mises on the top surface is shown in Fig. 18. The location of plastic hinges is clearly visible (the area where reduced stress reached the yield stress of material). Evaluation of the results follows.

Limit acceleration

$$a_{yL} = LF_L \cdot a_y = 2.64 \cdot 9.81 = 25.90\ m.s^{-2}$$

Allowable acceleration

$$a_{yALL} = \frac{a_{yL}}{S_f} = \frac{25.90}{2} = 12.95\ m.s^{-2}$$

Strength condition

$a_y = 9.81\ m.s^{-2} \quad \leq \quad a_{yALL} = 12.95\ m.s^{-2}$ -----> Satisfies

**The calculation result shows that the hood is properly designed and it satisfy on the calculation load case $a_z=1 \cdot g=9,81\ m.s^{-2}$ *and* $a_y=1 \cdot g=9.81\ m.s^{-2}$ (*LC*=5+)**

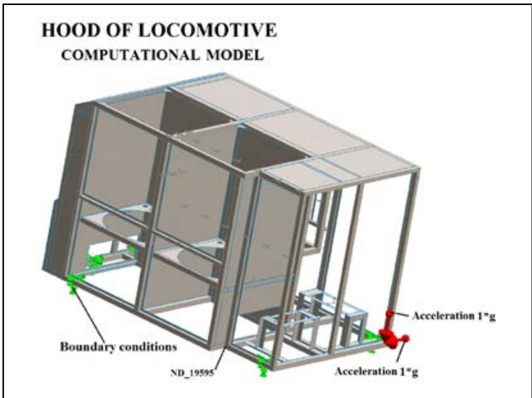


*Fig. 15:* *Numerical model – LC 5+.*

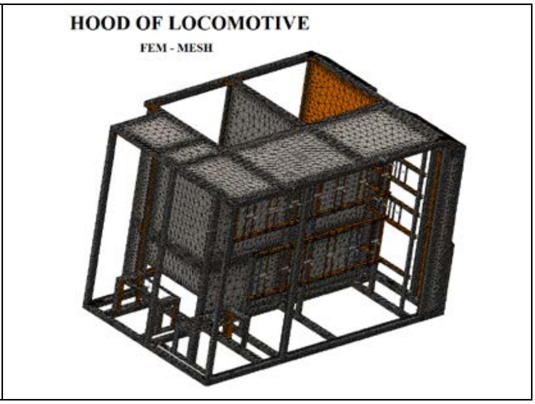


*Fig. 16:* *FEM mesh – LC 5+.*

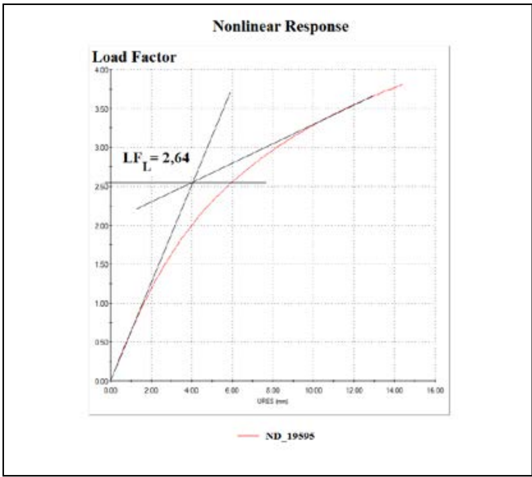


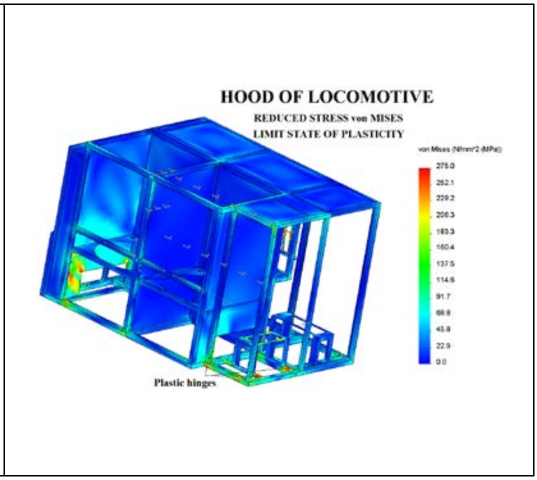


***Fig. 17:*** *Equilibrium curve–LC 5+.* ***Fig. 18:*** *Reduced stress Misses–LC 5+.*

**Longitudinal acceleration $a_x$ = 29.43 m/s$^2$ (LC 4-)**

Results and evaluation of the strength of hood for the longitudinal acceleration are shown in this chapter. Detailed description of numerical analysis and evaluation of the strength is presented in chapter vertical acceleration. The limit acceleration of the numerical model is found in this chapter. The computational model is shown in Fig. 19. FEM mesh is created by shell element SHELL3T (Fig. 20). The numerical model is exposed to acceleration *$a_z=1\cdot g=9.81\ m.s^{-2}$ and $a_x=3\cdot g=29.43\ m.s^{-2}$*. Limit state of plasticity is reached in the 47$^{th}$ step. The value of limit load factor is $LF_L$ = 1.03 (see equilibrium curve in Fig. 21). Deformed model with drawn reduced stress von Mises on the top surface is shown in Fig. 22. The location of plastic hinges is clearly visible (the area where reduced stress reached the yield stress of material). Evaluation of the results follows.

Limit acceleration

$$a_{xL} = LF_L \cdot a_x = 1.03 \cdot 29.43 = 30.31\ m.s^{-2}$$

Allowable acceleration

$$a_{xALL} = \frac{a_{xL}}{S_f} = \frac{30.31}{2} = 15.16\ m.s^{-2}$$

Strength condition

$$a_x = 29.43\ m.s^{-2} \quad \nleq \quad a_{xALL} = 15.16\ m.s^{-2}$$ -----> Does not satisfy

**<u>The calculation result shows that the hood is not properly designed and it does not satisfy on the calculation load case $a_z$=1·g=9.81 m.s$^{-2}$ and $a_x$=3·g=29.43 m.s$^{-2}$ (LC=4-)</u>**

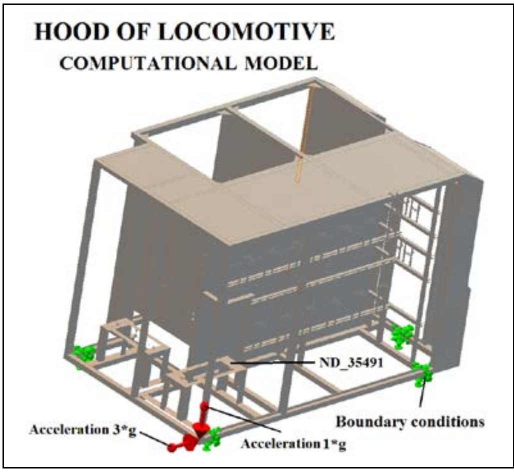


*Fig. 19:* Numerical model – LC 4-.

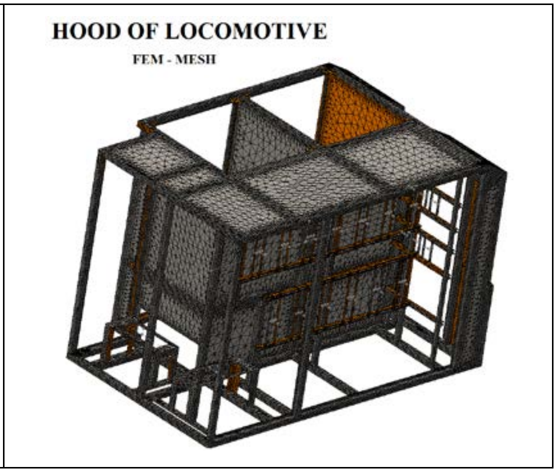


*Fig. 20:* FEM mesh – LC 4-.

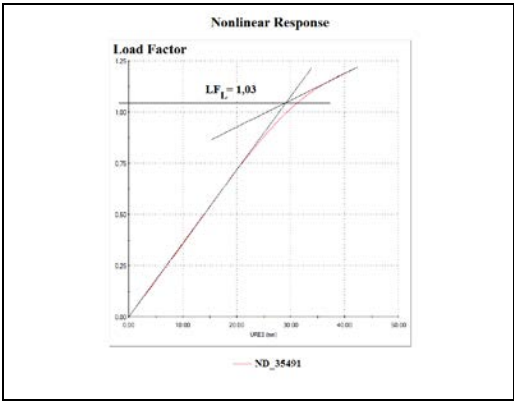


***Fig. 21:*** *Equilibrium curve–LC 4-.*

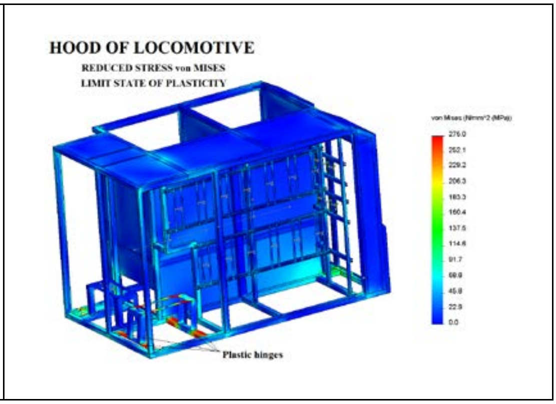


***Fig. 22:*** *Reduced stress Misses–LC 4-.*

## Longitudinal acceleration $a_x$ = 29.43 m/s$^2$ - other parts of the hood (LC 4-)

Results and evaluation of the strength other parts of the hood for the longitudinal acceleration are shown in this chapter. The parts of hood with a small load carrying capacity (see Fig. 22) are reinforced so that they cannot influence the rest of the structure. Detailed description of numerical analysis and evaluation of the strength is presented in chapter vertical acceleration. The limit acceleration of the numerical model is found in this chapter. The computational model is shown in Fig. 23. FEM mesh is created by shell element SHELL3T (Fig. 24). The numerical model is exposed to acceleration $a_z=3 \cdot g=29.43\ m.s^{-2}$ *and* $a_x=9 \cdot g=88.29\ m.s^{-2}$*.* Limit state of plasticity is reached in the 49$^{th}$ step. The value of limit load factor is $LF_L$ = 0.6 (see equilibrium curve in Fig. 25). Deformed model with drawn reduced stress von Mises on the top surface are shown in

Fig. 26 and Fig. 27. The location of plastic hinges is clearly visible (the area where reduced stress reached the yield stress of material). Evaluation of the results follows.

Limit acceleration

$$a_{xL} = LF_L \cdot a_x = 0.6 \cdot 88.29 = 52.97\ m.s^{-2}$$

Allowable acceleration

$$a_{xALL} = \frac{a_{xL}}{S_f} = \frac{52.97}{2} = 26.49\ m.s^{-2}$$

Strength condition

$a_x = 29.43\ m.s^{-2} \quad \nleq \quad a_{xALL} = 26.49\ m.s^{-2}$ -----> Does not satisfy

**<u>The calculation result shows that the hood is not properly designed and it does not satisfy on the calculation load case $a_z$=1·g=9.81 m.s$^{-2}$ and $a_x$=3·g=29.43 m.s$^{-2}$ (LC=4-)</u>**

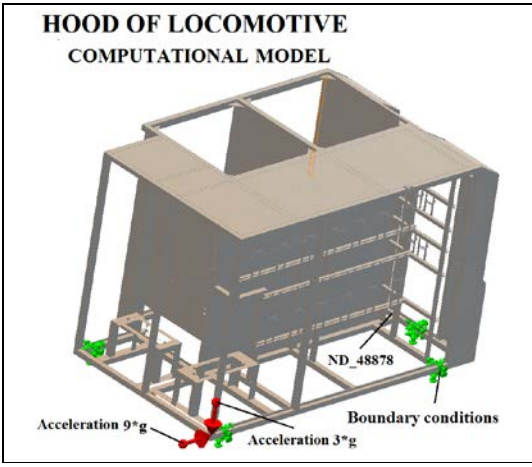


***Fig. 23:*** *Numerical model – LC 4-.*

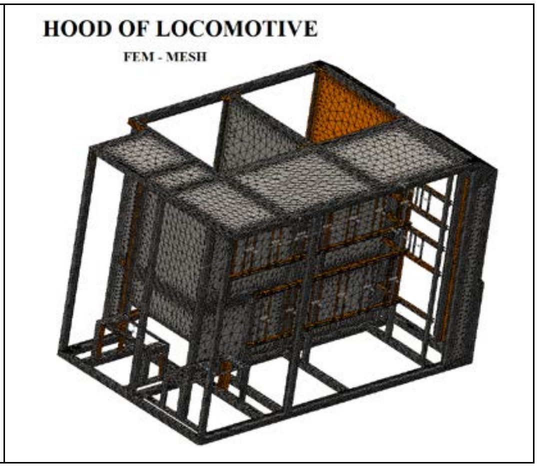


***Fig. 24:*** *FEM mesh – LC 4-.*

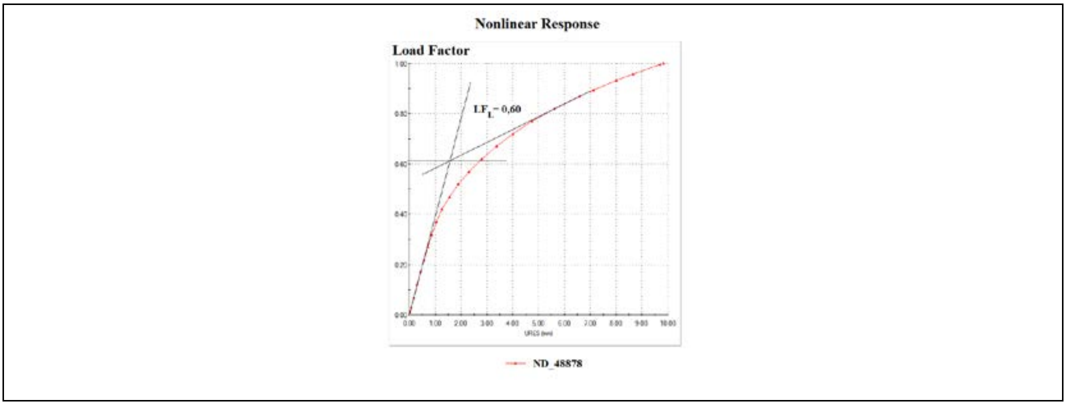


***Fig. 25:*** *Equilibrium curve – LC 4-.*

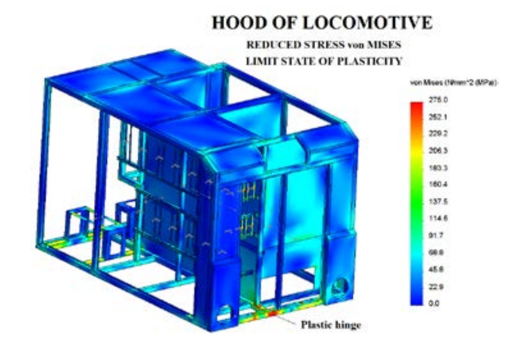


**Fig. 26:** *Reduced stress Misses–LC 4-.*

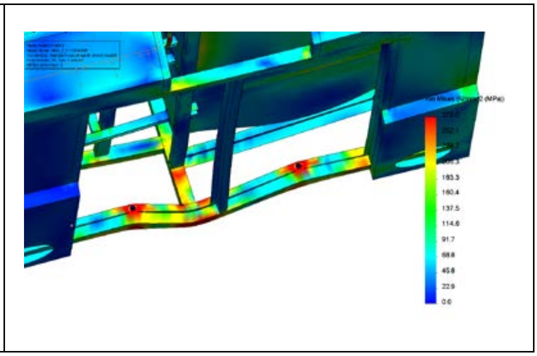

**Fig. 27:** *Detail of plastic hinges–LC 4-.*

## 7. Conclusion

The strength of hood was evaluation by two methods. The first methodology is anchored in ČSN EN 12663-1 [1]. Evaluation of strength of hood was performed on the basis of pseudo elastic reduced stress on the TOP area or BOTTOM area. This method does not properly evaluate the influence of loss of stability and plasticity of carrying capacity structure.

The second methodology is nonlinear numerical analysis GMNA (Geometrically and Materially Nonlinear Analysis). The second methodology was used on basis of methods of modern science and technology. The real limit states (plasticity and loss of stability) were investigated using nonlinear numerical analyses GMNA. Evaluation of strength of hood was performed on the basis of real limit state of construction.

The results are shown in chapter 5 and chapter 6. The calculation result shows that the hood is not properly designed and it does not satisfy on the calculation load case. These results are used to perform modification hood. Strength of new construction will be again checked by nonlinear numerical analysis GMNA.

*Předloženo: 31. 5. 2013*

## References

[1] ČSN EN 12663 - 1. *Železniční aplikace – Pevnostní požadavky na konstrukce skříní kolejových vozidel- Část 1: Lokomotivy a vozidla osobní dopravy.* Česká technická norma. Český normalizační institut, Říjen 2010.

[2] Paščenko, P., Švanda, P.: *„Stability of Simply Supported Spherical Cap Subjected to External Pressure"*, Journal of Machine Manufacturing, vol. XLIX, no. E3-E5, Special Triple Edition 2009, s. 120-123. ISSN: 0016-8580, 2009.

[3] ČSN 73 1401. *Navrhování ocelových konstrukcí.* Česká technická norma. Český normalizační institut, 1998.

[4] Paščenko, P., Tomek, P., Schwarz, S., Zelenka, J.: *Kostra kapoty železniční lokomotivy (etapa 1, etapa 2)*. Výpočtová zpráva. Univerzita Pardubice, Dopravní Fakulta Jana Pernera, Katedra Mechaniky, Materiálů a Částí Strojů, 2012.

## Resumé

## KONTROLA PEVNOSTI KAPOTY DIESEL ELEKTRICKÉ LOKOMOTIVY

Petr TOMEK, Doubravka STŘEDOVÁ

Tento článek představuje dvě metodiky pro vyhodnocení pevnosti kostry kapoty železniční lokomotivy. Kostra kapoty podléhá ustanovením normy pro železniční aplikace ČSN EN 12663–1[1]. První metoda je zakotvená v normě pro železniční aplikace ČSN EN 12663–1[1]. Tato metoda je založená na principu vyhodnocení tzv. pseudo-elastických napětí. Druhá metoda využívá výsledky nelineární numerické analýzy GMNA. Použití druhé metody vychází z poznatků současné vědy a techniky. Pevnost konstrukce je potom vyhodnocena ze skutečného mezního stavu. Výsledky v tomto článku jsou použity pro změny stávajícího konstrukčního řešení kapoty.



## Summary

## STRENGTH CHECK OF THE CABIN OF DIESEL ELETRIC LOCOMOTIVE

Petr TOMEK, Doubravka STŘEDOVÁ

This article presents two methods for evaluating strength of hood railway locomotives. The hood is subject to the standards for railway applications ČSN EN 12663-1 [1]. The first method is anchored in the standard for rail applications ČSN EN 12663-1 [1]. This method is based on the principle of evaluation of the pseudo-elastic stress. The second method uses the results of nonlinear numerical analyzes GMNA. The second method is based on the knowledge of modern science and technology. Structural strength is then evaluated from the real limit state. The results in this article are used for the structural design modifications to the existing hood.



## Zusammenfassung

## NACHKRITISCHES VERHALTUNG DIE ZYLINDRISCHE SCHALE

Petr TOMEK, Doubravka STŘEDOVÁ

Dieser Artikel stellt zwei Methoden für die Festigkeitsbewertung von Haubenskelett von Lokomotive vor. Das Haubenskelett unterliegt den Normen für Bahnanwendungen ČSN EN 12663-1 [1]. Die erste Methode wird in der Norm für Bahnanwendungen ČSN EN 12663-1 [1] angeführt. Dieses Verfahren ist auf dem Prinzip der Auswertung der Pseudo-elastische Spannung aufgebaut. Die zweite Methode verwendet die Ergebnisse der nichtlinearen numerischen Analysen GMNA. Die zweite Methode ist auf den Erkenntnissen der modernen Wissenschaft und Technologie aufgebaut. Konstruktionsfestigkeit wird dann von dem tatsächlichen Grenzzustand evaluiert werden. In diesem Artikel ausgeführte Ergebnisse sind für die Änderungen an dem bestehenden Haubenskelett verwendet.